







# Geotechnical properties of some kaolinite-rich Brazilian Vertisols

Gustavo Magalhães Nunes Barbosa<sup>(1)</sup> , Eduardo Antonio Gomes Marques<sup>(2)</sup> , João Carlos Ker<sup>(3)</sup> , Igor Rodrigues de Assis<sup>(3)\*</sup> , Tony Jarbas Ferreira Cunha<sup>(4)</sup>  and Luciano da Silva Souza<sup>(5)</sup> 

<sup>(1)</sup> Universidade Federal de Viçosa, Programa de Pós-Graduação em Solos e Nutrição de Plantas, Viçosa, Minas Gerais, Brasil.

<sup>(2)</sup> Universidade Federal de Viçosa, Departamento de Engenharia Civil, Viçosa, Minas Gerais, Brasil.

<sup>(3)</sup> Universidade Federal de Viçosa, Departamento de Solos, Viçosa, Minas Gerais, Brasil.

<sup>(4)</sup> Empresa Brasileira de Pesquisa Agropecuária, Embrapa Semiárido, Petrolina, Pernambuco, Brasil.

<sup>(5)</sup> Universidade Federal do Recôncavo da Bahia, Centro de Ciências Agrárias, Ambientais e Biológicas, Cruz das Almas, Bahia, Brasil.

**ABSTRACT:** Vertisols presenting kaolinite codominance or prevalence were already reported in several countries worldwide. However, the literature has few studies focused on investigating the influence of this clay mineral in soil geotechnical behavior. This study aimed to carry out the characterization of Vertisols in Bahia State, Brazil, to understand the influence of physical, chemical, and mineralogical properties on their geotechnical behavior, as these soils have high natural fertility and have been used for agricultural activity, but with great risk due to their physical and geotechnical properties. Six Vertisols were selected, three located in Juazeiro County (Semiarid region) and the other three in Recôncavo region. Geotechnical characterization of selected soils was carried out in their respective diagnostic horizons by determining properties such as granulometric curve, Atterberg limits, clay activity, linear expansion coefficient, compaction capacity, cohesion ( $c$ ), and internal friction angle ( $\phi$ ) of saturated soils. Soil expansion potential was associated with expansive clay contents and clay content in each soil sample. The best soil compaction efficiency was observed for kaolinitic Vertisol, which presented greater void ratio reduction and higher density due to moisture increase. In addition,  $c$  increased as kaolinite content also increased and decreased as clay content increased in soils presenting similar mineralogy. On the other hand,  $\phi$  was influenced mainly by granulometry since higher sand and gravel levels enabled higher  $\phi$ , regardless of clay type.

**Keywords:** semiarid, kaolinite, expansive soils, *Vertissolo*.

\* Corresponding author:  
E-mail: igor.assis@ufv.br

**Received:** February 25, 2021

**Approved:** May 28, 2021

**How to cite:** Barbosa GMN, Marques EAG, Ker JC, Assis IR, Cunha TJF, Souza LS. Geotechnical properties of some kaolinite-rich Brazilian Vertisols. Rev Bras Cienc Solo. 2021;45:e0210022. <https://doi.org/10.36783/18069657rbc20210022>

**Editors:** José Miguel Reichert  and João Tavares Filho 

**Copyright:** This is an open-access article distributed under the terms of the Creative Commons Attribution License, which permits unrestricted use, distribution, and reproduction in any medium, provided that the original author and source are credited.



## INTRODUCTION

Geotechnical properties of expansive soils have been investigated in several regions worldwide, mainly due to damage caused by expansion and shrinkage processes to civil construction (Chen, 1988; Driscoll and Crilly, 2000; Hakari and Puranik, 2010, 2011; Paiva et al., 2016). The potential of these soils to expand is mainly associated with the incidence of expansive clay minerals, such as smectites, in them. These minerals, in their turn, can also affect other geotechnical parameters, such as soil cohesion, internal friction angle (Taha et al., 2000; Miao et al., 2002; Cokca et al., 2004; Rahardjo et al., 2004; Heping et al., 2005; Kumor, 2008; Ye et al., 2010; Adejumo et al., 2012) and compaction ability (Gan et al., 1988; Ene and Okagbue, 2009; Gheorghie et al., 2013; Capurro et al., 2014).

Vertisols in Brazil are mainly found in regions whose terrain, climate, or origin material are conducive to the genesis and conservation of expansive clay minerals, such as the Semiarid and Recôncavo Baiano regions. Vertisols in these regions present highly varying granulometric properties that lead to textures ranging from medium to very clayey (Jacomine et al., 1979; Lima, 2014). With respect to mineralogy, in addition to soils presenting prevalence of smectite in their clay fraction, there are also soils presenting codominance of smectite and kaolinite and even prevalence of kaolinite (Lima, 2014), which is a non-expansive clay mineral.

Kaolinite-rich expansive soils are mentioned in several studies conducted in different regions worldwide, such as El Salvador (Yerima et al., 1985, 1987) and Sudan (Yousif et al., 1988). However, the literature has few studies focused on investigating the influence of these clay minerals on the geotechnical properties of these soils.

Understanding the influence of mineralogy on the geotechnical behavior of Vertisols in the Semiarid and Recôncavo regions can help explain these soils' formation and conservation and their influence on geotechnical properties. It can be done by investigating the extent to which the formation of non-expansive clay minerals affects its expansiveness, or, yet, whether there are physical or chemical properties capable of enhancing the expansion capacity of these soils, even of the ones presenting kaolinite prevalence.

A better understanding of the Vertisols' properties is important because of the constant increase in the use of these soils, mainly because of their high natural fertility. However, these soils have severe limitations mainly due to their physical and geotechnical properties. In soil science, great emphasis is placed on studies of the physical properties of these soils, but there are no geotechnical characterization studies, which highlights the importance of a better understanding of the impacts caused by their use.

This study aimed to present the results of the geotechnical properties of Vertisols in the Semiarid and the Recôncavo Baiano regions, Brazil, to improve the understanding of the influence of chemical, physical, and mineralogical properties on the expansion potential, compaction ability, cohesion, and internal friction angle of these soils.

## MATERIALS AND METHODS

### Selected soils and study sites

Six expansive soils were herein selected: three (P01, P02, and P03) in Juazeiro County, Semiarid region of Bahia State, and the other three (P04, P05, and P06) in the Recôncavo region (Figure 1). Those soils were selected based on their representativeness of the Vertisols geographical distribution, visual characterization, and associated geotechnical problems observed in the Semiarid region. Soils located in the Semiarid region are derived from limestone belonging to Caatinga Formation in flat terrain. In contrast, those located in Recôncavo region are derived from the gray-green shales of Candeias Formation (Table 1), in flat (P04 and P06) and wavy (P05) terrains.

Selected soils were classified based on the World Reference Base (IUSS Working Group WRB, 2015) (Table 1) by considering the morphological, physical, and chemical properties of their profiles. Geotechnical characterization was performed in the most expressive

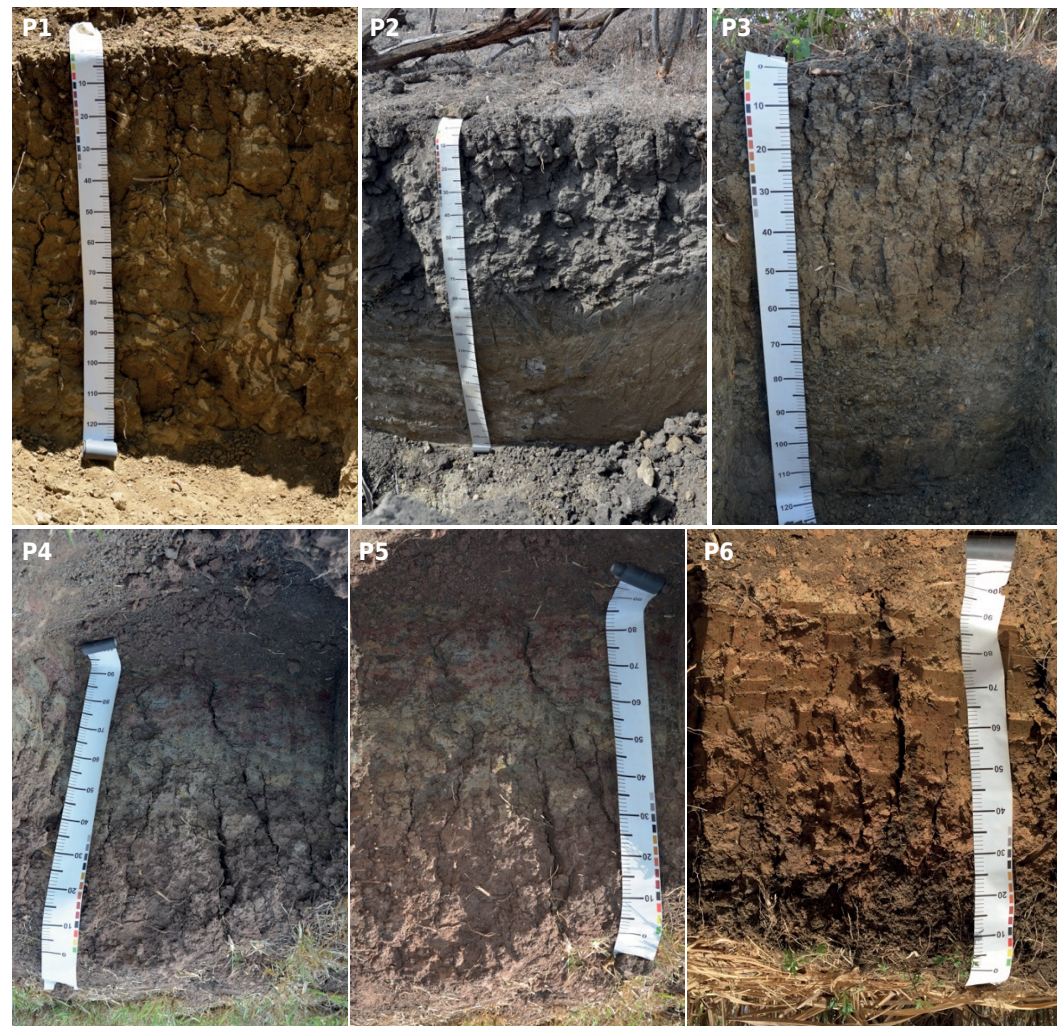


**Figure 1.** Soil profiles sampled in Juazeiro County, Semiarid region of Bahia State (P01, P02, and P03), and Recôncavo region (P04, P05, and P06).

**Table 1.** Profiles location, classification of, and data about the analyzed horizons and physical environment

Profile	Geographic coordinate	Soil classification <sup>(1)/(2)</sup>	Hor	Layer	Geology	Origin material
				m		
P01	9° 23' 33" S 40° 24' 49" W	Vertisol Haplic Aric / <i>Vertissolo Háplico Órtico endosalino</i>	Biv2	0.30-0.80	Caatinga Formation	Results from changes in limestone
P02	9° 30' 30" S 40° 22' 52" W	Vertisol Sodic Aric / <i>Vertissolo Háplico Sáfico solódico</i>	Biv2	0.25-0.80	Caatinga Formation	Results from changes in limestone
P03	9° 43' 47" S 40° 21' 44" W	Vertisol Haplic calcaric / <i>Vertissolo Háplico Órtico típico hipocarbonático</i>	Biv2	0.24-0.50 <sup>+</sup>	Caatinga Formation	Results from changes in limestone
P04	12° 37' 05" S 38° 40' 18" W	Vertisol Haplic calcaric / <i>Vertissolo Háplico Órtico típico com carbonato</i>	Biv	0.42-0.73	Candeias Formation	Shales with limestone lenses
P05	12° 32' 23" S 38° 37' 48" W	Vertisol Haplic Aric / <i>Vertissolo Háplico Órtico típico</i>	Biv	0.18-0.38	Candeias Formation	Shales with limestone lenses
P06	12° 29' 03" S 38° 38' 49" W	Vertisol Sodic Aric / <i>Vertissolo Háplico Órtico solódico</i>	Bivn	0.25-0.48	Candeias Formation	Shales with limestone lenses

<sup>(1)</sup> World Reference Base System of Soil Classification (IUSS Working Group WRB, 2015); <sup>(2)</sup> Brazilian Soil Classification System. Hor: analyzed horizon; VXo: Ortíc HAPLÍC VERTÍSOLO; VXz: Sáfico HAPLÍC VERTÍSOLO. Geologic database: Geological Survey of Brazil (CPRM). Hor: horizon.

diagnostic horizons of each soil (Table 1), whose physical (Table 2), chemical (Table 3), and mineralogical (Table 4) attributes had been previously determined. All selected horizons presented vertic properties, such as prismatic structure formation, cracks,

**Table 2.** Physical properties of the six Vertisols sampled in Bahia State

Profile	CSSa	SSSa	$\delta a$
	m <sup>2</sup> g <sup>-1</sup>		g cm <sup>-3</sup>
P01	95.19	1.98	2.68
P02	159.37	0.18	2.68
P03	238.46	17.79	2.74
P04	99.41	28.93	2.73
P05	124.88	18.38	2.75
P06	155.93	28.69	2.77

CSSa: clay-specific surface area; SSSa: silt-specific surface area;  $\delta a$ : specific mass of soil grains (<2.0 mm).

**Table 3.** Chemical properties of the six Vertisols sampled in Bahia State

Property	Profile					
	P01	P02	P03	P04	P05	P06
pH(H <sub>2</sub> O)	8.0	7.87	8.30	8.21	6.44	5.23
pH(KCl)	6.4	6.51	6.82	6.97	5.02	3.58
P (mg dm <sup>-3</sup> )	1.70	9.10	0.30	64.70	27.50	1.10
Ca <sup>2+</sup> (cmol <sub>c</sub> dm <sup>-3</sup> )	27.17	28.62	55.44	31.73	19.53	19.69
Mg <sup>2+</sup> (cmol <sub>c</sub> dm <sup>-3</sup> )	3.32	4.58	4.90	6.77	9.59	12.67
K <sup>+</sup> (cmol <sub>c</sub> dm <sup>-3</sup> )	0.08	0.24	0.04	0.09	0.40	0.20
Na <sup>+</sup> (cmol <sub>c</sub> dm <sup>-3</sup> )	0.46	4.37	0.22	0.12	0.09	0.31
Al <sup>3+</sup> (cmol <sub>c</sub> dm <sup>-3</sup> )	0.00	0.00	0.00	0.00	0.00	10.70
H+Al (cmol <sub>c</sub> dm <sup>-3</sup> )	0.80	0.70	0.70	1.20	4.10	16.30
SB (cmol <sub>c</sub> dm <sup>-3</sup> )	31.03	37.81	60.61	38.71	29.61	32.87
CTC <sub>pH7</sub> (cmol <sub>c</sub> dm <sup>-3</sup> )	31.83	38.51	61.31	39.91	33.71	49.17
V (%)	97.50	98.20	98.90	97.00	87.80	66.80
M (%)	0.00	0.00	0.00	0.00	0.00	24.60
PST (%)	1.44	11.35	0.37	0.30	0.25	0.63
COT (dag kg <sup>-1</sup> )	0.41	0.47	0.75	0.63	1.30	0.85
Carb. eq. (g kg <sup>-1</sup> )	4.62	9.19	80.65	33.49	1.00	0.00
P-rem (mg L <sup>-1</sup> )	21.50	40.40	26.00	23.50	29.30	7.40

SB: sum of exchangeable bases; CEC<sub>pH7</sub>: Cation Exchange Capacity at pH 7.0; V: base saturation index; m: aluminum saturation index; COT: total organic carbon. Carb. eq.: equivalent calcium carbonate; P-rem: remaining phosphorus.

**Table 4.** Mineralogical composition of clay, silt, and sand fractions in Bahia State's Vertisols

Profile	Clay		Silt		Sand	
	Prevalent stage	Other identified stages	Prevalent stage	Other identified stages	Prevalent stage	Other identified stages
P01	Kt	Mt, S-OH, I	Qz	Fd	Qz	Fd
P02	S (Mt, B/N)	I, Kt, Fd	Qz	Fd	Qz	Fd
P03	S (Mt, B/N)	Kt, I	Qz	Fd	Qz	Fd
P04	S (Mt), Kt	I	Qz	Fd, I, Kt, S	Qz	Fd
P05	S (Mt), Kt	I	Qz	Fd, I, Kt, S	Qz	Fd, Kt
P06	S (Mt), Kt	I	Qz	Fd, I, Kt	Qz	Fd, I

S: smectite; Mt: montmorillonite; B/N: beidelite / nontronite; S-OH: smectite with hydroxy between layers; I: Illite; Kt: kaolinite; Fd: feldspar; Qz: quartz.

and slickensides. Clay- and silt-specific areas were determined based on water vapor saturation, according to the method described in Quirk (1955). The specific mass of soil grains or particle density was determined by the volumetric flask method (Teixeira et al., 2017). All physical, chemical, and mineralogical analyses were performed according to Teixeira et al. (2017). Soil pH in water and in KCl at a soil:solution ratio of 1:2.5; P, Na<sup>+</sup>, K<sup>+</sup> were extracted by Mehlich-1; Ca<sup>2+</sup>, Mg<sup>2+</sup>, and Al<sup>3+</sup> were extracted by KCl 1 mol L<sup>-1</sup>; H + Al was extracted by calcium acetate 0.5 mol L<sup>-1</sup> at pH 7.0; total organic carbon was determined by wet oxidation (Walkley-Black, 1934).

## Geotechnical characterization

### Particle-size curve

Deformed soil samples were sieved in 2.0 mm mesh to separate fine soil (<2.0 mm) from gravels (>2.0 mm) to determine the particle-size curve (ABNT, 1984a). Gravels were divided into seven classes based on sieving in mechanical stirrer using 50, 37.5, 25, 19, 9.5, and 4.75-mm mesh sieves; their masses were determined after drying oven at 105 °C, for 24 h.

Fine soil samples (70 g) were chemically and physically dispersed in an electric stirrer for 15 min using 125 mL of sodium hexametaphosphate (0.078 mol L<sup>-1</sup>) to determine sand, silt, and clay content. After the stirring process was over, samples were sieved (0.075 mm mesh) to separate the coarsest sand fractions from the rest of the sample. Particles larger than 0.075 mm were further subdivided by sieving in mechanical stirrer (1.18, 0.6, 0.425, 0.25, and 0.15 mm meshes).

Silt and clay contents were determined through sedimentation. Particles smaller than 0.075 mm were transferred to 1,000 mL beakers, manually stirred, and subjected to readings in densimeter at the following times: 0.25, 0.5, 1, 2, 4, 8, 15, 30, 60, 120, and 240 min, as well as 8, 24, 36, 72, and 96 h. Gravel (>2.0 mm), coarse (2.0-0.6 mm), medium (0.6-0.2 mm) and fine sand (0.2-0.06 mm), silt (0.06-0.002 mm), and clay (<0.002 mm) contents were calculated after the particle-size curve was determined (ABNT, 1995).

### Atterberg limits

Deformed samples were sieved in 0.42 mm mesh, and their coarsest fraction was discarded to determine the Atterberg limits. The shrinkage limit (SL) was determined based on the water volume necessary to fill the pores of the soil paste dried in the oven at 105 °C, for 24 h. Next, saturated soil pastes (<0.42 mm) were prepared and transferred to the shrinking capsule and air-dried until their color changed. After this, the samples were oven-dried, weighed and their volumes were determined based on the water volume displaced when paraffin-waterproofed samples at 70 °C were immersed in water (Donagemma et al., 2011). Water mass referring to the porosity of the saturated dry paste was calculated based on ABNT (1982).

The gravimetric moisture required for molding soil threads (<0.42 mm) with approximately 10 cm in length and 3 mm in diameter was considered as plastic limit (PL). Threads were manually molded on the glass surface, and the moisture allowing the onset of cracks when cylinders reached 3.0-mm diameter was considered PL.

Saturated soil pastes (<0.42 mm) were prepared to determine liquid limit (LL); they were transferred to the brass cup of the LL determination apparatus, with a maximum thickness of approximately 1.0 cm. After this procedure was over, a groove was made in the soil with the aid of a chisel by applying consecutive strokes, in free fall from the height of 1.0 cm, at the frequency of two strokes per second, until 1.0 cm groove closure was reached. The test was repeated until five different moisture points were achieved at the interval between 15 and 35 strokes. Subsequently, linear adjustment was applied to

the points, and LL was estimated as the moisture referring to 25 strokes (ABNT, 1984b). Plasticity index ( $PI = LL - PL$ ) and clay activity ( $Ac = PL / \% \text{ clay}$ ) were calculated based on LL and PL results (Nelson et al., 2015).

### **Linear expansion coefficient**

The Coefficient of Linear expansion (COLE) was determined based on the difference in volume between saturated and oven-dried soil (105 °C). Non-deformed samples were collected in volumetric rings (5.0 cm in diameter and 2.5 cm in height), which were saturated in a container filled with a 2.3 cm water layer. After the saturation process, the samples were reduced to the same volume as the ring and dried in the oven for 48 h. After the oven-drying process was over, sample volume was determined based on the water volume displaced when soil waterproofed with paraffin at 70 °C was immersed in it (Donagemma et al., 2011). Results were used to calculate the apparent specific mass of saturated ( $\delta'$ ) and oven-dried soil at 105 °C ( $\delta$ ), as well as the void indices of saturated ( $\epsilon'$ ) and dry ( $\epsilon$ ) soils, wherein  $\epsilon = [1 - (\delta/\delta_a)] \times 100$ .

COLE was determined based on the association between  $\delta'$  and  $\delta$ , through equation 1 (Nelson et al., 2015).

$$COLE = \left( \frac{\delta}{\delta'} \right)^{1/3} - 1 \quad \text{Eq. 1}$$

### **Proctor compaction test**

Compaction test was applied to samples of P01, P02, P04, P05, and P06 using Proctor cylinder (1,000 cm<sup>3</sup>) and socket (2.5 kg). The adopted free fall spacing was 30.5 cm (ABNT, 1986). Soil samples used in this test were fragmented and sieved (4.8 mm mesh). Sieved subsamples were collected, moistened, homogenized, and left to equilibrate for 24 h. Each sub-sample was moistened with a water increment equal to 2 % of mass basis moisture. The number of subsamples was equal to the one necessary to reach three points before maximum compaction (dry branch) and two points after it (wet branch).

Each subsample was subjected to compaction in three layers, based on the application of 26 strokes in each one of them. Apparent specific masses of the analyzed soils, and their respective moisture, were determined at the end of compaction to find the compaction curve associated with the apparent specific mass of the compacted soil ("y" axis) and the compaction moisture ("x" axis). After the test was over, the points recorded for each sample were subjected to quadratic adjustment, and maximum points were estimated based on the second-order derivative of the curve. Estimated values of ordinates "x" and "y" were considered as optimum moisture for maximum soil compaction ( $\omega_c$ ) and maximum apparent soil density ( $\Upsilon_c$ ), respectively.

Results were used to calculate the soil void index for maximum soil compaction state ( $\epsilon_c$ ), wherein  $\epsilon_c (\%) = [1 - (\Upsilon_c / \delta_a)] \times 100$ . Relative apparent specific masses between  $\Upsilon_c$  and  $\delta'$  ( $\Upsilon_r'$ ), as well as between  $\Upsilon_c$  and  $\delta$  ( $\Upsilon_r$ ), were also calculated based on the following formula:  $\Upsilon_r (\%) = (\Upsilon_c / \delta) \times 100$ .

Soil saturation index (Is) at maximum compaction state was also estimated based on the association between  $w_c$  and saturated soil moisture ( $\omega'$ ), wherein  $Is (\%) = (\omega_c / \omega') \times 100$ .

### **Direct shear of saturated soil**

Direct shear tests were only carried out at soil saturation state (ASTM, 2000) since it was not possible performing them in specimens at field moisture state because they presented strong cohesion. Non-deformed specimens collected in square-base metallic molds (dimensions of 5 × 5 × 2 cm) were used in the test. They were collected in soil blocks pre-moistened through capillarity and molded to the shape of the metallic mold.

Specimens were water-saturated for 24 h and densified by applying normal stresses (50, 100, and 200 kPa) for four hours before the test. Variations in specimens' height were recorded with digital extensometer during the densification process to determine specimens' apparent specific mass ( $\delta_{cp}$ ) and void index ( $\epsilon_{cp}$ ) after compaction. Compaction degrees (CD) recorded for each normal stress were calculated based on  $\delta_{cp}$  results, by using the following formula:  $CD (\%) = [(\delta' - \delta_{cp})/\delta'] \times 100$ .

Saturated specimens were subjected to shearing at a speed of  $0.1 \text{ mm min}^{-1}$ ; shear stress was computed with the aid of a load cell. After the tests - based on all three normal stresses - were over, maximum shear stress points ( $\tau_c$ ) were subjected to linear adjustment to find the saturated soil cohesion ( $c$ ), referring to the shear stress without the application of normal stress, which was estimated based on the adjusted line. The internal friction angle ( $\phi$ ) was determined based on the slope of the line.

### Statistical analysis

All analyses performed during the geotechnical characterization, except for the one estimated based on linear adjustments, were performed in triplicate. Results were subjected to descriptive statistical analysis in the Sisvar<sup>®</sup> software to determine central tendency (mean) and dispersion measurements (variance, coefficient of variation, and maximum and minimum values).

## RESULTS

### Granulometry, Atterberg limits, and COLE

Overall, the analyzed soil samples have shown fine granulometry prevalence, mainly the ones collected in Recôncavo region (P04, P05, and P06), whose source material was shale. Profiles P05 and P06 have shown total sand contents lower than 4 %, whereas the clay contents were 62 and 81 %, respectively (Figures 2e and 2f).

Profile P05 presented approximately 10 % of fine gravel, composed of shale fragments with an advanced weathering stage. Since shale is a fine-grained rock, the weathering of this material contributes to the formation of low-sand-content soils, as seen in the granulometric curve discontinuity at the gravel-to-coarse sand transition point (Figure 2e). Although P04 was clayey, its granulometric distribution was more uniform than P05 and P06 since it presented approximately 11 % of fine sand and 30 % silt (Figure 2d).

If compared with the Recôncavo profiles, the semiarid profiles (P01, P02, and P03) presented greater variation in granulometric distribution - clay contents ranged from 350 to  $680 \text{ g kg}^{-1}$  in P01 and P02, respectively (Figures 2a, 2b, and 2c). Granulometric distribution also affected moisture values related to the Atterberg limits of the investigated soils. Recôncavo soils - which were more clayey and presented lower sand contents - shown higher moisture values than Semiarid soils, which, in their turn, presented the lowest limits and plasticity indices in P01 and P02, whereas P03 presented the closest values to those of Recôncavo soils (Table 5). Despite these differences, all soil samples recorded high LL and low PL values, which resulted in high plasticity index (Nelson et al., 2015).

Recôncavo soil samples have shown clay activity ( $C_a$ ) close to the one expected for soils presenting illite mineral phase (0.9), as shown in table 5 (Nelson et al., 2015). However, the mineralogy of these soils comprises a mix of mineral phases that show smectite-kaolinite (Sm-Kt) codominance. Therefore, the herein recorded  $C_a$  values can be interpreted as intermediate values between the ones expected for montmorillonite (1.5 - 7.2) and kaolinite (0.33 - 0.46) (Nelson et al., 2015).

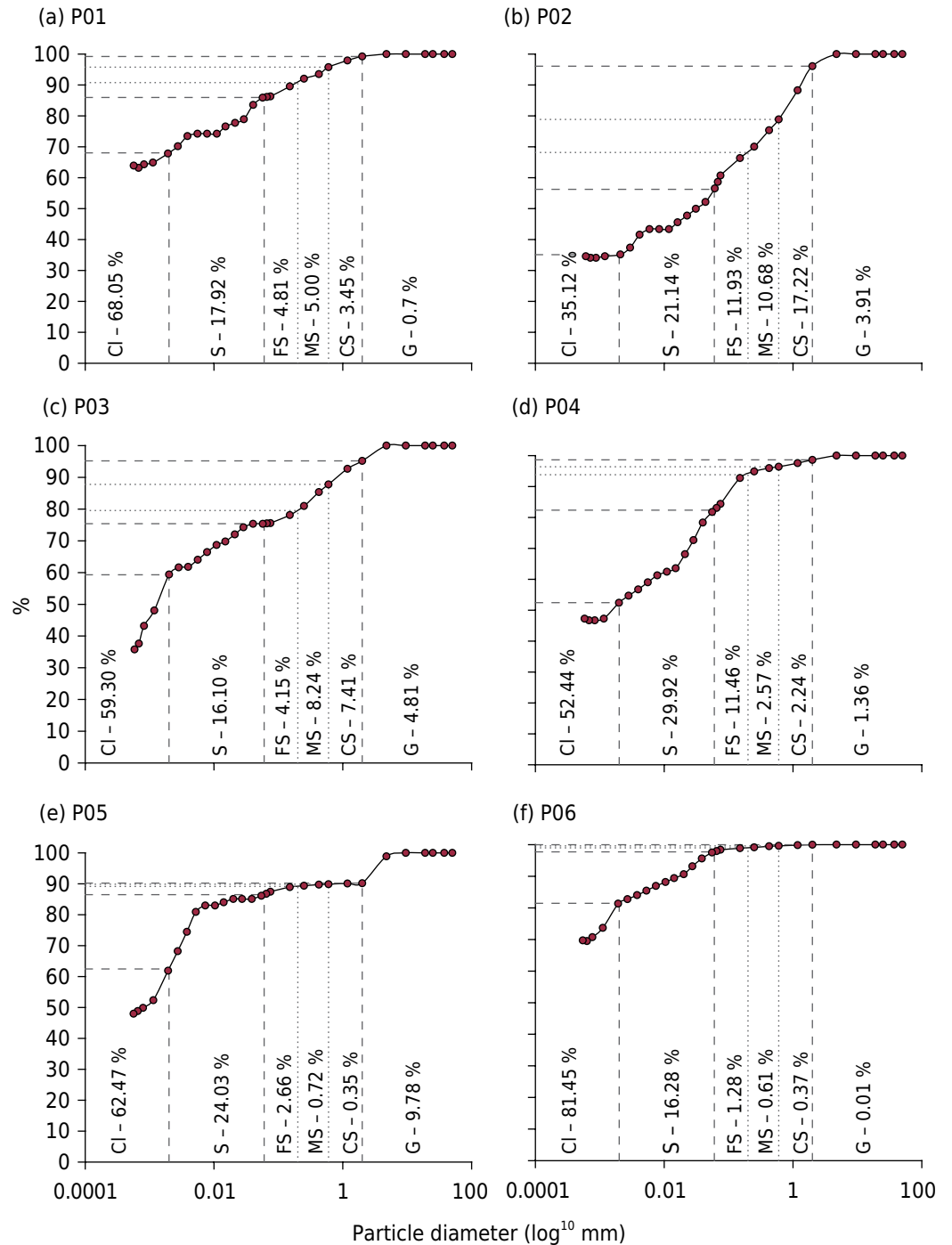


**Figure 2.** Granulometric curves of Vertisols in Bahia State (CI: clay; S: silt; FS: fine sand; MS: medium sand; Cs: coarse sand; G: gravel).

Clay activity ( $C_a$ ) in P01 (Table 5) was in agreement with that expected for soils presenting kaolinite prevalence.  $C_a$  values observed for P02 and P03 (Table 5) were lower than the ones expected for soils presenting montmorillonite prevalence. This outcome has shown that the other lesser expansive mineral phases have contributed to  $C_a$  decrease, even in small proportions. Different clay types collected in P01 and P02 (Table 4) - which presented the highest and lowest  $C_a$ , respectively (Table 5) - can explain how these two soils presented similar LL, PL, PP, and SL values, despite their different granulometry (Table 5). Clay activity ( $C_a$ ) also influenced the potential of Semiarid Vertisols to expand since soils presenting the highest (P03) and lowest (P01)  $C_a$  have shown the highest and lowest COLE, respectively (Table 6). Overall, Recôncavo Vertisols - which are more clayey than Semiarid Vertisols - recorded the highest  $\varepsilon$  and  $\delta$  values, as well as the lowest  $\delta'$



values (Table 6). The great difference between  $\delta$  and  $\delta'$  resulted in higher COLE values than the mean values recorded for Semiarid Vertisols (Table 6).

### Proctor compaction test

Soil samples collected in the Semiarid region (Figures 3a and 3b) presented higher  $\gamma_c$  and lower  $\omega_c$  values than those recorded for soil samples collected in Recôncavo region (Figures 3c, 3d, and 3e). Recôncavo soil samples, in their turn, presented wider compaction curves, and this finding indicated a lower response to increased compaction

**Table 5.** Atterberg limits and clay activity of some kaolinite-rich Brazilian Vertisols

Feature	Mean	$\sigma^2$	CV	Mx	Mn
%					
P01 - Vertisol Haplic Aric/Vertissolo Háplico Órtico endosalino - Juazeiro-BA					
LL (% mass) <sup>(1)</sup>	52.22	-	-	-	-
PL (% mass)	23.91	0.0805	1.19	24.29	23.61
PI (% mass)	28.31	0.0806	1.00	28.61	27.93
SL (% mass)	14.97	0.3225	3.79	15.40	14.32
Ca	0.4159	0.0000	1.00	0.4204	0.4105
P02 - Vertisol Sodic Aric/Vertissolo Háplico Sálido solódico - Juazeiro-BA					
LL (% mass) <sup>(1)</sup>	52.39	-	-	-	-
PL (% mass)	21.94	0.2730	2.38	22.37	21.28
PI (% mass)	30.44	0.2730	1.72	31.11	30.02
SL (% mass)	12.27	0.9463	7.92	13.39	11.65
Ca	0.8669	0.0003	1.72	0.8859	0.8548
P03 - Vertisol Haplic calcaric/Vertissolo Háplico Órtico típico hipocarbonático - Juazeiro-BA					
LL (% mass) <sup>(1)</sup>	64.20	-	-	-	-
PL (% mass)	30.34	1.2961	3.75	31.78	28.83
PI (% mass)	33.86	1.2961	3.36	35.37	32.42
SL (% mass)	17.19	0.7492	5.03	18.06	16.33
Ca	0.5771	0.0004	3.36	0.5965	0.5467
P04 - Vertisol Haplic calcaric/Vertissolo Háplico Órtico típico com carbonato - São Francisco do Conde-BA					
LL (% mass) <sup>(1)</sup>	66.67	-	-	-	-
PL (% mass)	30.06	0.1180	1.14	30.23	29.54
PI (% mass)	36.61	0.1180	0.94	37.12	36.44
SL (% mass)	15.55	0.1300	2.32	15.95	15.26
Ca	0.6981	0.0000	0.94	0.7079	0.6948
P05 - Vertisol Haplic Aric/Vertissolo Háplico Órtico típico - São Sebastião do Passé-BA					
LL (% mass) <sup>(1)</sup>	69.70	-	-	-	-
PL (% mass)	30.55	2.3545	5.02	32.04	29.11
PI (% mass)	39.15	2.3545	3.92	40.59	37.66
SL (% mass)	16.13	0.0912	1.87	16.44	15.84
Ca	0.6267	0.0007	3.92	0.6497	0.6029
P06 - Vertisol Sodic Aric/Vertissolo Háplico Órtico solódico - Santo Amaro-BA					
LL (% mass) <sup>(1)</sup>	94.94	-	-	-	-
PL (% mass)	40.32	0.6878	2.06	41.46	39.51
PI (% mass)	54.61	0.6878	1.52	55.43	53.48
SL (% mass)	17.94	0.0674	1.45	18.19	17.67
Ca	0.6688	0.0001	1.52	0.6806	0.6566

<sup>(1)</sup> Feature estimated through linear adjustment.  $\sigma^2$ : variance; CV: coefficient of variation; Mx: maximum value; Mn: minimum value; PL: plasticity limit; PI: plasticity index; SL: shrinking limit; Ca: clay activity.

**Table 6.** Apparent specific mass, void index and COLE recorded for some kaolinite-rich Brazilian Vertisols

	Mean	$\sigma^2$	CV	Mx	Mn
	%				
P01 - Vertisol Haplic Aric/ <i>Vertissolo Háplico Órtico endosalino</i> - Juazeiro-BA					
$\delta$ (g cm <sup>-3</sup> )	1.79	0.0000	0.35	1.79	1.78
$\delta'$ (g cm <sup>-3</sup> )	1.34	0.0003	1.28	1.32	1.35
$\varepsilon$ (% , volume)	33.32	0.0548	0.70	33.56	33.09
$\varepsilon'$ (% , volume)	53.64	4.8229	4.09	55.92	51.54
COLE	0.1002	0.0000	5.00	0.1057	0.0959
P02 - Vertisol Sodic Aric/ <i>Vertissolo Háplico Sáfico solódico</i> - Juazeiro-BA					
$\delta$ (g cm <sup>-3</sup> )	1.96	0.0000	0.44	1.97	1.95
$\delta'$ (g cm <sup>-3</sup> )	1.42	0.0014	2.58	1.39	1.46
$\varepsilon$ (% , volume)	26.95	0.1060	1.21	27.22	26.59
$\varepsilon'$ (% , volume)	49.11	2.8995	3.47	51.01	47.72
COLE	0.1119	0.0001	9.36	0.1191	0.0999
P03 - Vertisol Haplic calcaric/ <i>Vertissolo Háplico Órtico típico hipocarbonático</i> - Juazeiro-BA					
$\delta$ (g cm <sup>-3</sup> )	1.96	0.0049	3.57	2.03	1.89
$\delta'$ (g cm <sup>-3</sup> )	1.26	0.0005	1.78	1.29	1.25
$\varepsilon$ (% , volume)	28.60	6.4981	8.91	30.93	25.88
$\varepsilon'$ (% , volume)	56.57	0.6569	1.43	57.35	55.73
COLE	0.1568	0.0000	4.58	0.1637	0.1493
P04 - Vertisol Haplic calcaric/ <i>Vertissolo Háplico Órtico típico com carbonato</i> - São Francisco do Conde-BA					
$\delta$ (g cm <sup>-3</sup> )	1.78	0.0014	2.08	1.82	1.75
$\delta'$ (g cm <sup>-3</sup> )	1.17	0.0002	1.32	1.16	1.19
$\varepsilon$ (% , volume)	34.60	1.8608	3.94	36.04	33.33
$\varepsilon'$ (% , volume)	61.62	0.2821	0.86	62.22	61.22
COLE	0.1500	0.0001	4.99	0.1560	0.1416
P05 - Vertisol Haplic Aric/ <i>Vertissolo Háplico Órtico típico</i> - São Sebastião do Passé-BA					
$\delta$ (g cm <sup>-3</sup> )	1.76	0.0008	1.60	1.78	1.73
$\delta'$ (g cm <sup>-3</sup> )	1.20	0.0030	4.55	1.24	1.14
$\varepsilon$ (% , volume)	35.90	1.0568	2.86	37.07	35.17
$\varepsilon'$ (% , volume)	62.11	1.1073	1.69	63.00	60.95
COLE	0.1357	0.0004	14.89	0.1586	0.1203
P06 - Vertisol Sodic Aric/ <i>Vertissolo Háplico Órtico solódico</i> - Santo Amaro-BA					
$\delta$ (g cm <sup>-3</sup> )	1.85	0.0014	2.01	1.88	1.81
$\delta'$ (g cm <sup>-3</sup> )	1.04	0.0011	3.17	1.06	1.00
$\varepsilon$ (% , volume)	33.28	1.8068	4.04	34.77	33.17
$\varepsilon'$ (% , volume)	68.78	0.3321	0.84	69.30	68.16
COLE	0.2104	0.0003	8.24	0.2277	0.1930

$\sigma^2$ : variance; CV: coefficient of variation;  $\delta'$ : apparent specific mass of saturated soil;  $\delta$ : apparent specific mass of soil dried at 105 °C;  $\varepsilon$ : void index of soil dried at 105 °C;  $\varepsilon'$ : void index of saturated soil; COLE: coefficient of linear expansion.

than to increased humidity (Figures 3c, 3d, and 3e). In addition, soil samples collected in this region presented higher  $\varepsilon_c$ , ranging from 43.40 to 55.27 % - than soil samples collected in the semiarid region, whose  $\varepsilon_c$  values ranged from 34.66 to 38.53 % (Figures 3d and 3e).

Based on the comparison between values recorded for  $\Upsilon_c$  and the ones recorded for  $\delta$  and  $\delta'$ ,  $\Upsilon_c$  was in an intermediate position, since it was lower than  $\delta$  and higher than  $\delta'$ . This

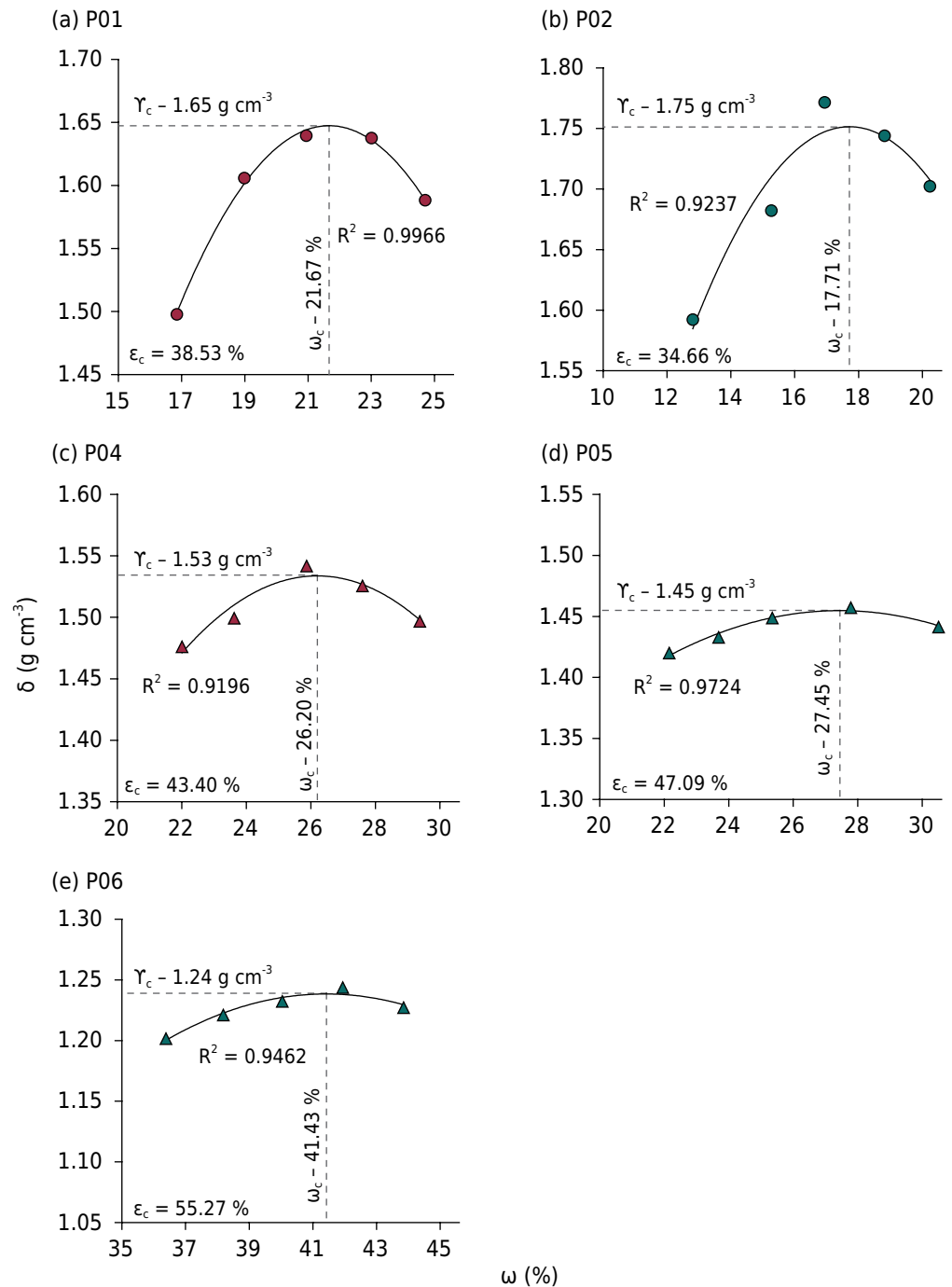


**Figure 3.** Compaction curve of Vertisols in Bahia State ( $\delta$ : apparent specific mass of dry soil;  $\omega$ : gravimetric moisture;  $\gamma_c$ : maximum apparent specific mass;  $\omega_c$ : optimal compaction moisture;  $\epsilon_c$ : void index of soil at maximum compaction stage).

behavior can be observed in values recorded for  $\Upsilon_r$  and  $\Upsilon_r'$ , since  $\Upsilon_r'$  was always higher than 100 % and  $\Upsilon_r$  was always lower than 100 % (Table 7). All soil samples reached the maximum compaction stage at approximately 50 % saturation moisture, as seen in the herein recorded saturation index ( $I_s$ ) values, ranging from 49.92 to 62.81 % (Table 7).

### Direct shear test application to saturated soil

Soil densification at normal stress of  $200 \text{ kgf cm}^{-2}$  was sufficient to reach  $\delta_{cp}$  values (Table 8) close to the ones recorded for  $\gamma_c$  (Figures 3b, 3c, 3d, and 3e) in P02, P04, P05, and P06. Profile P01 has greater resistance to densification, mainly from 100 to  $200 \text{ kgf cm}^{-2}$ , since it maintained  $\delta_{cp}$  (Table 8) lower than  $\gamma_c$  (Figure 3a).

**Table 7.** Compaction test applied to some kaolinite-rich Brazilian Vertisols

Feature	Mean	$\sigma^2$	CV	Mx	Mn
			%		
P01 - Vertisol Haplic Aric/Vertissolo Háplico Órtico endosalino - Juazeiro-BA					
$\Upsilon_r$ (%)	92.18	0.10	0.35	92.51	91.87
$\Upsilon_r'$ (%)	122.76	2.50	1.29	124.58	121.75
Is (%)	54.29	8.14	5.25	56.88	51.23
P02 - Vertisol Sodic Aric/Vertissolo Háplico Sálido solódico - Juazeiro-BA					
$\Upsilon_r$ (%)	89.45	0.16	0.44	89.78	89.01
$\Upsilon_r'$ (%)	122.99	9.90	1.82	125.54	119.48
Is (%)	51.44	8.90	5.80	54.40	48.44
P04 - Vertisol Haplic calcaric/Vertissolo Háplico Órtico típico com carbonato - São Francisco do Conde-BA					
$\Upsilon_r$ (%)	85.96	3.24	2.09	87.87	84.30
$\Upsilon_r'$ (%)	130.71	2.98	1.32	132.42	128.97
Si(%)	49.92	0.52	1.45	50.74	49.41
P05 - Vertisol Haplic Aric/Vertissolo Háplico Órtico típico - São Sebastião do Passé-BA					
$\Upsilon_r$ (%)	82.55	1.78	1.62	84.08	81.62
$\Upsilon_r'$ (%)	120.95	31.85	4.66	127.44	117.20
Is (%)	53.25	7.24	5.06	55.43	50.24
P06 - Vertisol Sodic Aric/Vertissolo Háplico Órtico solódico - Santo Amaro-BA					
$\Upsilon_r$ (%)	67.05	1.85	2.03	68.57	65.94
$\Upsilon_r'$ (%)	118.90	14.74	3.23	123.32	116.44
Is (%)	62.81	4.42	3.34	64.39	60.42

$\sigma^2$ : variance; CV: coefficient of variation;  $\Upsilon_r$ : specific mass ratio between compacted soil and the soil dried at 105 °C;  $\Upsilon_r'$ : apparent specific mass ratio between compacted and saturated soils; Is: soil saturation index at maximum compaction stage.

Although P01 was resistant to densification, it responded to normal stress increase by increasing shear strength. It presented the fourth largest  $\phi$ , after P03, P02, and P04 (in that order), as well as the highest cohesion value (Table 8). Although all the investigated soils responded to normal stress increase, they presented low friction angle (between 7.4 and 20.0°), which is expected to be observed in clayey soils (Cho et al., 2006).

The cohesion of saturated soil ( $c$ ) ranged from 2 to 19 kPa, which is often seen in clayey soils presenting low shear resistance (Adejumo et al., 2012). The highest  $c$  value was recorded for the Kaolinitic Vertisol (P01), which was followed by soils presenting Sm-Kt mineralogy (P04, P05, and P06) and, finally, by smectitic soils (P02 and P03), as shown in table 8.

### Correlation between geotechnical and physical-chemical properties of the soils

Several significant correlations were found between the variables studied (Table 9). We highlight the positive correlations between the Atterberg limits and the exchangeable Mg levels and a negative correlation with base saturation. The COLE index showed a significant and positive correlation with the variables  $Mg^{2+}$ , H+Al, SSSa, and  $\delta a$ . The  $Mg^{2+}$  and  $\delta a$  variables were the ones that showed the highest amounts of significant correlations with the geotechnical variables, showing that they are important to differentiate the mechanical behavior of these soils.

**Table 8.** Direct shear test applied to some kaolinite-rich Brazilian Vertisols

N	Ss	CD	$\delta_{cp}$	Pt	$\phi$	c
kPa	kgf cm <sup>-2</sup>	%	g cm <sup>-3</sup>	%	°	kgf cm <sup>-2</sup>
P01 - Vertisol Haplic Aric/Vertissolo Háplico Órtico endosalino - Juazeiro-BA						
50	0.29	3.06	1.51	43.54		
100	0.48	5.80	1.57	41.61	14.70	0.19
200	0.69	5.95	1.58	41.14		
P02 - Vertisol Sodic Aric/Vertissolo Háplico Sállico solódico - Juazeiro-BA						
50	0.22	3.11	1.60	40.11		
100	0.38	11.13	1.74	34.84	19.96	0.03
200	0.76	15.70	1.81	32.29		
P03 - Vertisol Haplic calcárico/Vertissolo Háplico Órtico típico hipocarbonático - Juazeiro-BA						
50	0.20	6.65	1.36	50.49		
100	0.38	15.20	1.54	43.70	19.97	0.02
200	0.74	24.05	1.67	38.92		
P04 - Vertisol Haplic calcárico/Vertissolo Háplico Órtico típico com carbonato - São Francisco do Conde-BA						
50	0.28	3.11	1.30	52.50		
100	0.44	11.16	1.47	46.11	18.23	0.11
200	0.77	15.58	1.52	44.49		
P05 - Vertisol Haplic Aric/Vertissolo Háplico Órtico típico - São Sebastião do Passé-BA						
50	0.23	6.42	1.43	47.86		
100	0.31	11.72	1.50	45.42	13.02	0.09
200	0.59	16.51	1.59	42.31		
P06 - Vertisol Sodic Aric/Vertissolo Háplico Órtico solódico - Santo Amaro-BA						
50	0.09	7.82	1.15	58.39		
100	0.23	13.32	1.23	55.53	7.36	0.05
200	0.30	18.47	1.32	52.36		

N: normal stress; Ss: shear stress; CD: compaction degree;  $\delta_{cp}$ : apparent specific mass of the specimen;  $\epsilon_{cp}$ : void index of the specimen;  $\phi$ : internal friction angle of saturated soil; c: cohesion of saturated soil.

**Table 9.** Result of the correlation analysis between the geotechnical variables and the variables of chemical and physical characterization of the soils

	pH		Mg <sup>2+</sup>	Na <sup>+</sup>	H+Al	SSSa	$\delta a$	V
	H <sub>2</sub> O	KCl						
LL	-0.84*	-0.83*	0.94*	-0.46	0.93*	0.81	0.89*	-0.93*
PL	-0.76	-0.75*	0.89*	-0.59	0.86*	0.86*	0.93*	-0.86*
PI	-0.89*	-0.87	0.96*	-0.36	0.95*	0.75	0.85*	-0.95*
SL	-0.50	-0.52	0.62	-0.84*	0.60	0.76	0.86*	-0.59
Ca	-0.09	-0.02	0.20	0.70	0.08	0.06	0.01	-0.07
$\delta$	0.26	0.24	-0.31	0.60	-0.12	-0.32	-0.19	0.20
$\delta'$	0.70	0.68	-0.87*	0.68	-0.79	-0.93*	-0.91*	0.79
$\epsilon$	-0.41	-0.39	0.50	-0.73	0.30	0.52	0.43	-0.37
$\epsilon'$	-0.75	-0.73	0.90*	-0.69	0.79	0.90*	0.91*	-0.81*
COLE	-0.67	-0.66	0.82*	-0.42	0.83*	0.84*	0.88*	-0.80
Yr (%)	0.92*	0.91*	-0.95*	0.35	-0.97*	-0.72	-0.88	0.98*
Yr' (%)	0.75	0.79	-0.44	-0.06	-0.60	0.19	-0.25	0.64
Is (%)	-0.87	-0.90*	0.70	-0.29	0.94*	0.34	0.57	-0.93*

\* Significant at the 0.05 level of significance.

## DISCUSSION

### Influence of granulometry and clay type on soil expansion potential

Quantifying the soil properties that define shrink-swell potential is essential to evaluate soil stability for agricultural use properly. The estimated shrink-swell potential cannot be accurate for all soil with only one method. This can be better determined by examining a combination of physical, chemical, and mineralogical soil properties (Thomas et al., 2000). The high number of significant correlations found reinforces this close relationship between these properties. All the analyzed soils have shown COLE values higher than 0.1; thus, their expansion capacity was classified as “very high” (Kariuki et al., 2004). Although all samples received the same classification, differences in COLE values between profiles have shown variation in their expansion potentials, which can be classified as  $P06 > P03 > P04 > P05 > P02 > P01$ , in decreasing order of expansion.

Expansion capacity can be mainly explained by clay content and type in the soil. Therefore, properties such as  $C_a$  and  $PI$  are often used to classify the soil expansion potential indirectly (Nayak and Christensen, 1971; Kariuki et al., 2004; Hakari and Puranik, 2010, 2011; Türköz and Tosun, 2011; Zumrawi, 2013). The use of these criteria led to different classifications for the investigated Vertisols.

If the association between clay content and  $C_a$  be considered, only P06 remained in the “very high” class, whereas P02 was positioned in the borderline area between “high” and “intermediate” classes, and the other profiles were positioned in the “high” class (Figure 4a). In this case, differences in  $C_a$  were counterbalanced by clay contents in the soil, such as the one in P01, whose expansion capacity was classified as “high” due to clay content higher than 68 %, despite its lower  $C_a$  (Figure 4a).

By considering the association between clay content and  $PI$ , most soils presented expansion potential classified as “very high”; only P01 and P02 were classified as “high” (Figure 4b). Even the least active clays ( $C_a < 0.5$ ) could have their expansion potential classified as high if they presented clay content higher than 70 %. Likewise, soils with  $PI > 35$  % can have their expansion potential classified as “very high”, if their clay content is higher than 25 %.

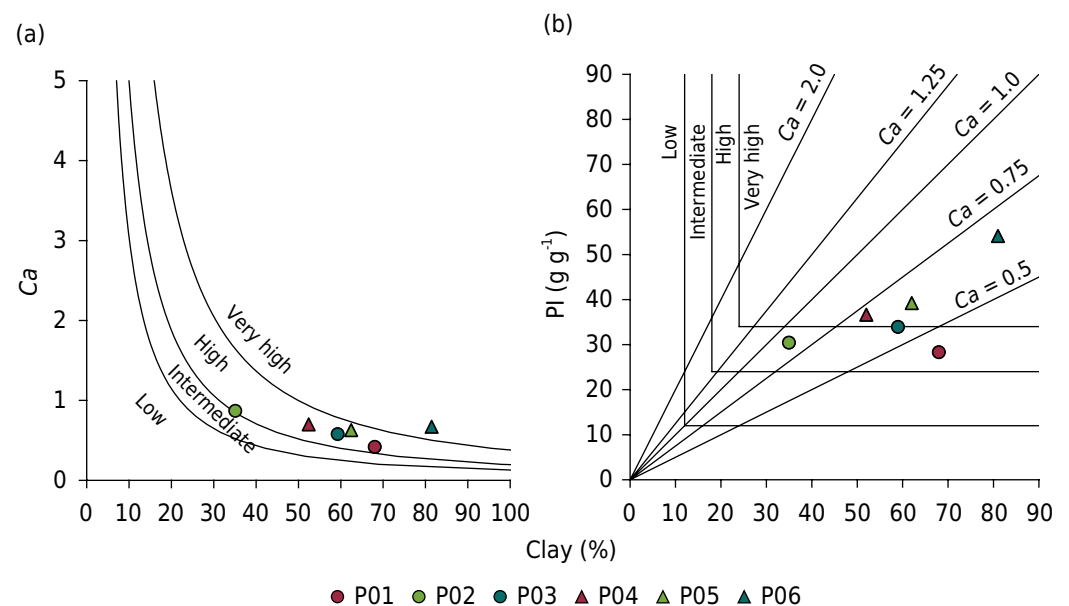


**Figure 4.** Classification of soil expansion potential based on charts proposed by (a) Seed et al. (1962) and (b) Carter and Bentley (1991) ( $C_a$  = clay activity).

Thus, the formation of vertic properties - which depend on soil expansion and shrinking processes - is limited to the incidence of expansive clays and clay content in the soil. Yet, shrink-swell potential in kaolinitic and mixed mineralogy soils are often more difficult to predict. Soils with equal amounts of kaolinite and montmorillonite behaved like montmorillonite soils, whereas soils with appreciable montmorillonite contents had wide ranges in swelling potentials (Thomas et al., 2000).

Profiles P01 and P02 are perfect examples of the association between clay content and type since they presented a clear influence of these two parameters on the expansive behavior of vertic soils. Both profiles developed vertic properties, such as prismatic structure, cracks, and slickensides, as well as received the same expansion potential classification (Figures 4a and 4b), although they presented completely different mineralogical properties (Table 4). If only Ca (Table 5) or clay expansion potential is considered (Figure 5), these two profiles represented the extremes since P01 presented the least active and least expansive kaolinitic clay. In contrast, the smectitic clay in P02 presented the highest Ca and the greatest expansiveness.

Thus, clay content higher than 68 % in P01 (Figure 2a) has promoted soil expansion potential, despite the prevalence of kaolinitic clay in it (Table 4). On the other hand, the expansion potential of the soil presenting smectitic clay in P02 (Table 4) was limited by sand and gravel contents higher than 40 % (Figure 2b).

The expansion potential of clays was also influenced by the cation type found in the smectite interlayer since higher  $\text{Ca}^{2+}$  content led to lower smectite expansion capacity. Because  $\text{Ca}^{2+}$  found in the smectite interlayer is divalent and has a smaller hydrated radius than  $\text{Na}^+$ , it enables lesser water absorption and, consequently, lower expansion and greater flocculation (Heil and Sposito, 1993; Paiva et al., 2016; Zumrawi and Eltayeb, 2016).

This behavior was observed in the difference in clay expansion potential between P05 and P06 (Figure 5). Although these two profiles have shown Sm-Kt mineralogy (Table 4), the higher  $\text{Ca}^{2+}$  content in P05 (Table 3) reduced clay expansion potential, which remained in the borderline region between high and intermediate expandability zones (Figure 5).

### Proctor compaction test

Concerning P02 and Recôncavo soils (P04, P05, and P06),  $\omega_c$  and  $\gamma_c$  of the investigated soils varied according to clay contents - reduction of clay contents increased  $\gamma_c$  and decreased  $\omega_c$  values (Figure 6).

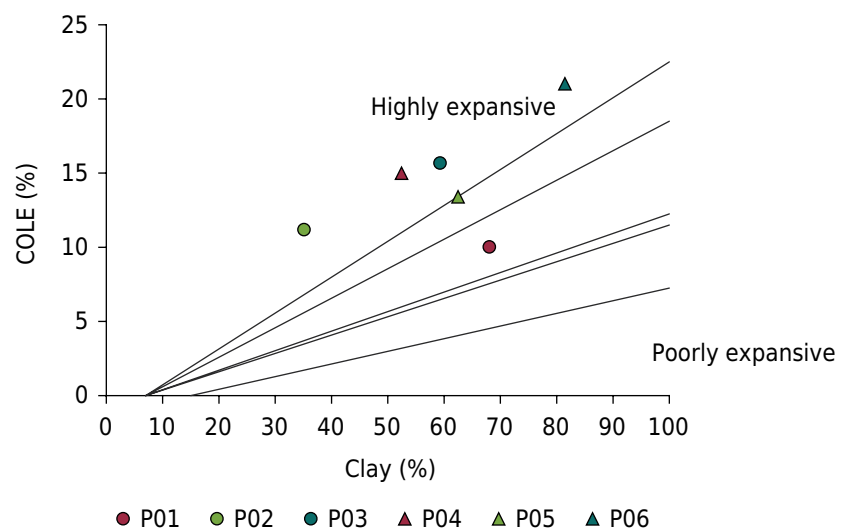


**Figure 5.** Classification of clay expansion potential (Lucian, 2016). COLE: coefficient of linear expansion [COLE (%) = COLE × 100].

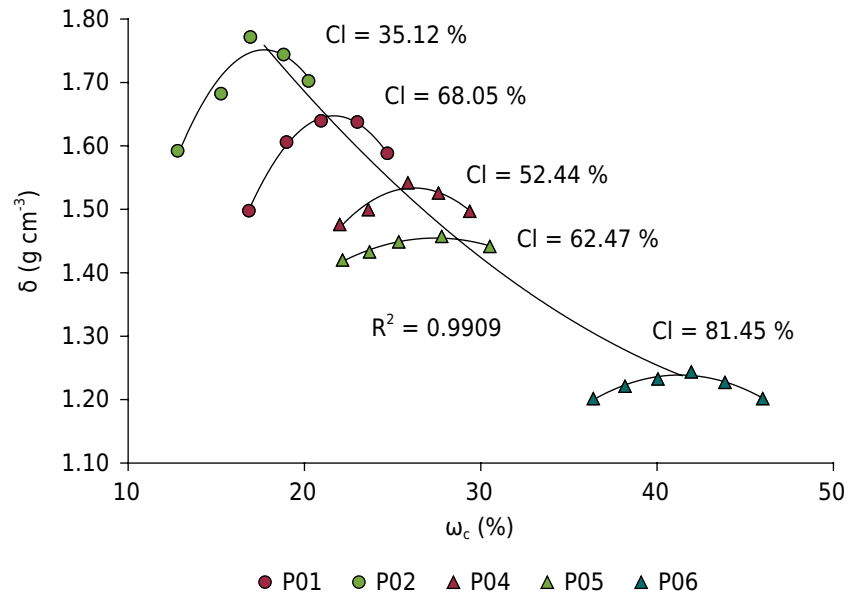


**Figure 6.** Quadratic adjustment of maximum points in the Proctor compaction curves ( $\delta$ : apparent specific mass of dry soil;  $\omega_c$ : gravimetric moisture; Cl: clay content).

In addition, higher clay contents resulted in wider curves (Figure 6), which was opposite to the behavior expected for clay soils, according to which soil structures present greater deformation as humidity increases. However, the behavior of soils subjected to compaction did not only depend on clay content but also on its type (Wagner et al., 1994). This factor evidenced clear behavioral differences between Vertisols and other clayey soils.

Behavioral differences associated with clay type were observed in P01, which presented the second highest  $\Upsilon_c$  and the narrowest compaction curve, although it had the second-highest clay content among all profiles (Figure 6). However, the variation in  $\Upsilon_c$  - based on the  $\omega_c$  observed in the investigated Vertisols - presented similar behavior to those presented by expansive soils worldwide, as shown in table 10 and figure 7.

The kaolinitic mineralogy of P01 (Table 4) enabled decreased void index (Figure 8b) and, consequently, it promoted  $\Upsilon_c$  closer to  $\delta$  (Figure 8a), in comparison to other soils. Therefore, the kaolinitic clay in P01 contributed to higher compaction efficiency among all the analyzed soils (Figures 8a and 8b). On the other hand, the lowest compaction efficiency was observed for P06; whose compacted sample shown a lesser increase in apparent specific mass (Figure 8a) and lesser reduction in the void index (Figure 8b) than the saturated sample.

The other profiles presented intermediate compaction efficiency; compacted samples shown reduced void indices (Figure 8b) and increased apparent specific masses (Figure 8a) in similar proportions. However, P02 and P05 presented similar compaction efficiency, although they had different physical and mineralogical properties. The low clay content observed (Figure 6) in P02 was counterbalanced by its high Ca (Table 5), and it limited soil compaction (Figure 8). On the other hand, the high clay content (Figure 6) observed in P05 enabled compaction due to clay expansion potential lower than the one observed in P02 (Figure 5).

### Direct shear

The  $\phi$  and  $c$  values observed for Vertisols in Bahia State were lower than the mean values observed for expansive soils worldwide (Figures 9a and 9b). However, they were within the range of values recorded for these soils (Table 9). This behavior indicates that Vertisols in Bahia State have lower shear resistance than other expansive soils.



**Table 10.** Geotechnical properties of expansive soils worldwide

Place	Sand	Silt	Clay	$\Upsilon_c$	$\omega_c$	$\phi$	c	Reference
	g kg <sup>-1</sup>			g dm <sup>-3</sup>	%	°	Kgf cm <sup>-2</sup>	
Australia	110	220	670	1.5	21.0	-	-	*
	30	260	710	1.6	25.5	-	-	*
	140	180	680	1.6	27.0	-	-	*
	200	230	570	1.6	28.0	-	-	*
	10	290	700	1.5	29.0	-	-	*
Botswana	-	-	47-58	1.2	22.0	-	-	*
Brazil	-	-	-	1.4	25.0	13.0	0.12	Simões de Oliveira et al. (2006)
Canada	28.0	42.0	30.0	1.8	16.0	25.5	0.10	Gan et al. (1988)
	-	-	-	1.6	23.9	23.4	0.17	Chowdhury (2013)
Chad	19.0	28.0	53.0	2.2	13.0	-	-	*
	14.0	34.0	52.0	1.7	18.6	-	-	*
China	-	-	-	-	-	24.6	0.78	Ye et al. (2010)
	6.7	68.5	24.8	-	-	21.3	0.33	Miao et al. (2002)
	-	-	-	-	-	15.6	0.37	Heping et al. (2005)
	-	-	-	-	-	44.0	0.41	Cokca et al. (2004)
	-	-	-	-	-	10.4	0.94	Kong and Tan (2000)
Ethiopia	4.0	38.0	56.0	1.5	23.0	-	-	*
Ghana	19.7	18.0	63.3	1.7	19.5	-	-	*
	38.3	15.2	46.5	1.8	17.5	-	-	*
India	6.0	54.0	40.0	1.3	35.0	-	-	*
	2.0	37.0	61.0	1.4	36.3	-	-	*
	7.0	41.0	52.0	1.3	28.0	-	-	*
	11.0	28.0	61.0	1.4	30.0	-	-	*
	6.0	54.0	40.0	1.3	35.0	-	-	*
	-	-	-	1.5	27.8	-	-	*
	28.0	32.0	40.0	1.7	20.0	-	-	*
	20.0	29.0	51.0	1.7	21.0	-	-	*
	-	-	-	1.4	21.0	-	-	*
	2.0	37.0	61.0	1.4	36.3	-	-	*
15.0	29.0	56.0	1.2	28.0	-	-	*	
Malaysia	-	-	-	-	-	21.0	0.04	Shanker and Maruthi (1989)
	-	-	-	-	-	26.6	0.59	Taha et al. (2000)
Nigeria	12.4	15.0	72.6	1.7	18.0	-	-	*
	20.0	5.0	75.0	1.6	19.2	-	-	*
	51.0	23.0	28.0	1.4	28.7	-	-	*
	-	-	-	1.4	24.3	-	-	*
	-	-	-	1.4	27.0	-	-	*
	-	-	-	-	-	4.0	1.22	Adejumo et al. (2012)
Poland	-	-	-	-	-	12.0	2.24	
	4.8	40.2	45.0	-	-	6.5	0.58	Kumor (2008)
Romania	25.8	21.9	52.3	-	-	9.5	0.51	Gheorghe et al. (2013)
	25.8	20.7	53.5	-	-	10.0	0.66	
Singapore	-	-	16.6	-	-	31.5	0.82	Rahardjo et al. (2004)
Tanzania	19.0	31.0	48.0	1.7	18.7	-	-	*
	15.0	43.0	42.0	1.7	10.2	-	-	*
	6.0	34.0	60.0	1.4	28.5	-	-	*
	45.0	20.0	35.0	1.6	22.0	-	-	*
	8.0	27.0	65.0	1.6	17.0	-	-	*
25.0	37.0	38.0	1.3	36.0	-	-	*	
Zambia	14.0	35.0	51.0	1.8	16.0	-	-	*

\* Values extracted from Gidigas and Gawu (2013);  $\Upsilon_c$ : maximum apparent specific mass;  $\omega_c$ : optimum compaction moisture;  $\phi$ : internal friction angle of saturated soil; c: cohesion of saturated soil.

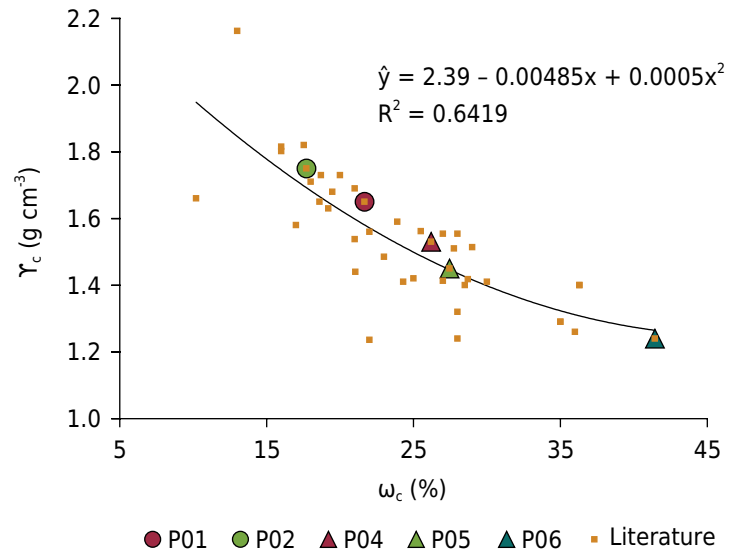


**Figure 7.** Relationship between optimum compaction moisture ( $\omega_c$ ) and a maximum apparent density ( $\gamma_c$ ) of Vertisols in Bahia State, in comparison to values recorded for expansive soils mentioned in the literature (Table 9).

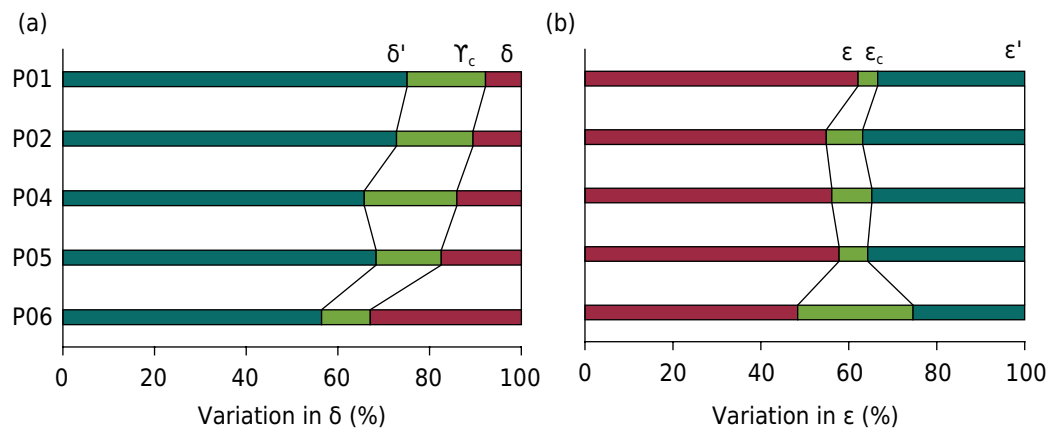


**Figure 8.** Variation in (a) apparent specific masses of soils dried in an oven at 105 °C ( $\delta$ ), as well as of saturated ( $\delta'$ ) and compacted ( $\gamma_c$ ) soils; and in (b) void indices of soils dried in an oven at 105 °C ( $\epsilon$ ), as well as of saturated ( $\epsilon'$ ) and compacted ( $\epsilon_c$ ) soils.

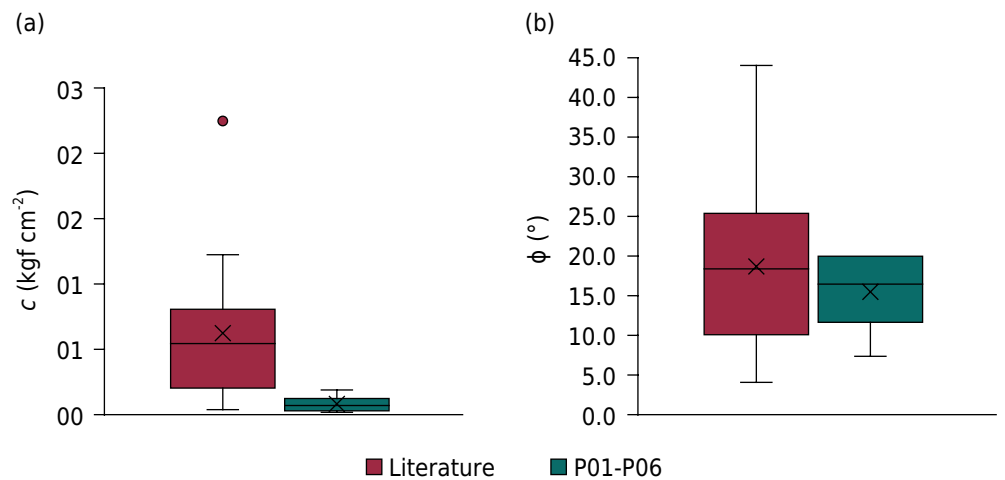


**Figure 9.** Cohesion (a) and friction angle (b) values recorded for Vertisols in Bahia State in comparison to values recorded for expansive soils mentioned in the literature (Table 9).  $c$ : cohesion;  $\phi$ : friction angle.

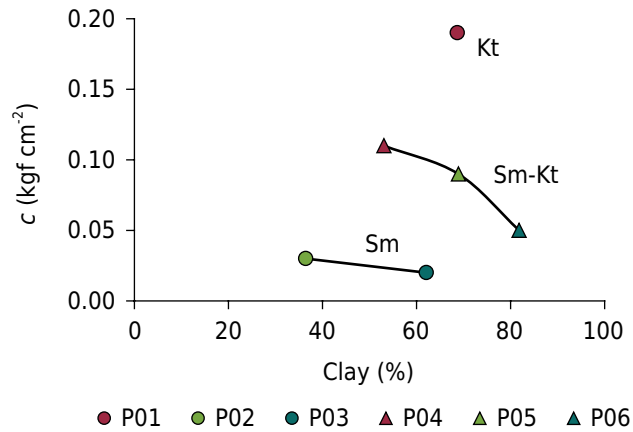


**Figure 10.** Variation in saturated soil cohesion ( $c$ ) in comparison to clay content and types (Kt: prevalence of kaolinite; Sm: prevalence of smectite; Sm-Kt: codominance of smectite and kaolinite).

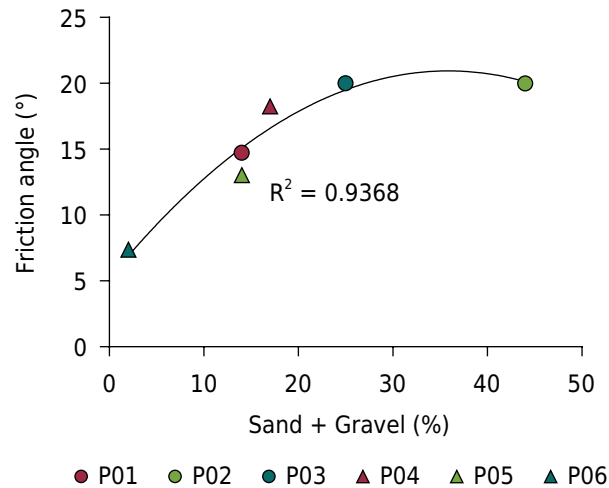


**Figure 11.** Association between the friction angle and the sums of sand and gravel contents.

Results observed for the investigated soils clarified that, just like soil expansion potential and compaction, clay granulometry and type were the main factors influencing the friction angle and cohesion of the investigated soils. Cohesion ( $c$ ) recorded the highest values as kaolinite contents at the predominant mineral stages of the clay increased. This outcome enabled dividing the investigated soils into three groups, namely: P01 (kaolinitic); P04, P05, and P06 (codominance of smectite and kaolinite); and P02 and P03 (smectitic), as shown in figure 10.

Therefore, the highest  $c$  value was recorded for P01, which was followed by Sm-Kt soils deriving from Recôncavo region and, finally, by smectitic soils deriving from the Semiárido region (Figure 10). This behavior results from smectites' ability to retain water in their interlayer, resulting in increases in the distance between clay particles and decreases of their interaction and, consequently, reducing soil cohesion.

Sm-Kt and smectitic soils also presented decreased  $c$  as clay contents increased, as expected since smectites enable lesser cohesion in saturated soils (Adejumo et al., 2012). Granulometry also influenced the internal friction angle of the investigated soils. Overall, the increased content of coarse particles, such as sand and gravel, hinders shear processes due to greater friction between particles (Cho et al., 2006). Thus, increased sand and gravel contents observed in the investigated soils were followed by increased  $\phi$  and stabilized between 24.61 % (P03) and 43.74 % (P02) (Figure 11). Thus, increased silt

and clay contents have led to decreased  $\phi$ , regardless of clay mineralogy. This outcome indicated that particle size distribution had a stronger influence on  $\phi$  than the clay type observed in the soil.

## CONCLUSIONS

Clay type and content in the soil were the aspects that most influenced the evaluated geotechnical properties. Soil potential to expand increased as clay content, and the incidence of smectite in the clay fraction also increased. The incidence of smectites and high clay content in the soil accounted for its increased expansion potential when kaolinite prevailed in the clay fraction.

Soil compaction efficiency was higher when kaolinite prevailed in the clay fraction, and it decreased as the content of smectite-rich clay increased. Increased clay content due to smectite prevalence or codominance reduced maximum apparent specific mass, increased optimum compaction moisture, and provided wider compaction curves than that of soils presenting lower clay contents or kaolinitic clay.





Kaolinite incidence increased saturated soil cohesion, which decreased as clay contents increased in soils presenting similar mineralogy. The internal friction angle of saturated soils has increased as sand and gravel contents increased. This angle also reduced as silt and clay contents increased, regardless of soil mineralogy. This outcome indicates that granulometry is more important than clay type for defining the internal friction angle of saturated soils.






These results are important for further studies on the soil capacity use for agricultural activities, including stability, given the peculiar characteristics of this soil class.






## ACKNOWLEDGEMENTS



This study was financed in part by the Coordenação de Aperfeiçoamento de Pessoal de Nível Superior - Brazil (CAPES) - Finance Code 001. The authors also would like to thank for Conselho Nacional de Desenvolvimento Científico e Tecnológico - Brazil (CNPq), Fundação de Amparo a Pesquisa de Minas Gerais (FAPEMIG), and the Departamento Nacional de Infraestrutura de Transportes (DNIT) for financial support. Furthermore, the authors are grateful to the editor and anonymous reviewers for their valuable suggestions, which improved the final quality of this study.

## AUTHOR CONTRIBUTIONS




**Conceptualization:**  Eduardo Antonio Gomes Marques (equal),  Gustavo Magalhães Nunes Barbosa (equal),  Igor Rodrigues de Assis (equal), and  João Carlos Ker (equal).



**Data curation:**  Gustavo Magalhães Nunes Barbosa (equal),  Igor Rodrigues de Assis (equal),  João Carlos Ker (equal),  Luciano da Silva Souza (equal), and  Tony Jarbas Ferreira Cunha (equal).




**Formal Analysis:**  Eduardo Antonio Gomes Marques (equal),  Gustavo Magalhães Nunes Barbosa (equal),  Igor Rodrigues de Assis (equal),  João Carlos Ker (equal), and  Luciano da Silva Souza (equal).



**Funding acquisition:**  Eduardo Antonio Gomes Marques (equal) and  Igor Rodrigues de Assis (equal).


**Investigation:**  Eduardo Antonio Gomes Marques (equal),  Gustavo Magalhães Nunes Barbosa (equal),  Igor Rodrigues de Assis (equal),  João Carlos Ker (equal),  Luciano da Silva Souza (equal), and  Tony Jarbas Ferreira Cunha (equal).



**Methodology:**  Gustavo Magalhães Nunes Barbosa (equal),  Igor Rodrigues de Assis (equal), and  João Carlos Ker (equal).

**Project administration:**  Igor Rodrigues de Assis (equal) and  João Carlos Ker (equal).

**Supervision:**  Eduardo Antonio Gomes Marques (equal),  Igor Rodrigues de Assis (supporting), and  João Carlos Ker (equal).

**Validation:**  João Carlos Ker (equal) and  Tony Jarbas Ferreira Cunha (equal).

**Writing - original draft:**  Eduardo Antonio Gomes Marques (equal).

**Writing - review & editing:**  Luciano da Silva Souza (equal) and  Tony Jarbas Ferreira Cunha (equal).

## REFERENCES

- Adejumo TW, Alhassan M, Boiko IL. Physico-mechanical properties of some major weak soils in Nigeria. *Electron J Geotech Eng*. 2012;17:2435-41.
- American Society for Testing and Materials - ASTM D6528. Standard test method for consolidated undrained direct simple shear testing of cohesive soils. West Conshohocken: ASTM International; 2000. <https://doi.org/10.1520/D6528-00>
- Associação Brasileira de Normas Técnicas - ABNT. NBR 6502: Rochas e Solos - Terminologia. Rio de Janeiro: ABNT; 1995.
- Associação Brasileira de Normas Técnicas - ABNT. NBR 7182: Solo - Ensaio de compactação. Rio de Janeiro: ABNT; 1986.
- Associação Brasileira de Normas Técnicas - ABNT. NBR NM 248: Agregados - Determinação da composição granulométrica. Rio de Janeiro: ABNT; 1984a.
- Associação Brasileira de Normas Técnicas - ABNT. NBR 6459: Solo - Determinação do limite de liquidez. Rio de Janeiro: ABNT; 1984b.
- Associação Brasileira de Normas Técnicas - ABNT. NBR 7251: Agregado em estado solto - Determinação da massa unitária. Rio de Janeiro: ABNT; 1982.
- Capurro EPG, Secco D, Reichert JM, Reinert DJ. Compressibilidade e elasticidade de um Vertissolo afetado pela intensidade de pastejo bovino. *Ciencia Rural*. 2014;44:e283288. <https://doi.org/10.1590/S0103-84782014000200014>
- Chen FH. Foundations on expansive soils. Amsterdam: Elsevier Scientific Publishing Company; 1988.
- Cho G-C, Dodds J, Santamarina JC. Particle shape effects on packing density, stiffness, and strength: natural and crushed sands. *J Geotech Geoenviron*. 2006;132:591-602. [https://doi.org/10.1061/\(ASCE\)1090-0241\(2006\)132:5\(591\)](https://doi.org/10.1061/(ASCE)1090-0241(2006)132:5(591))
- Chowdhury RH. Shear strength properties of compacted expansive soils. Regina, Canadá: University of Regina; 2013.
- Cokca E, Erol O, Armangil F. Effects of compaction moisture content on the shear strength of an unsaturated clay. *Geotech Geol Eng*. 2004;22:285-97. <https://doi.org/10.1023/B:GEGE.0000018349.40866.3e>
- Donagemma GK, Campos DVB, Calderano SB, Teixeira WG, Viana JHM. Manual de métodos de análise do solo. 2. ed. rev. Rio de Janeiro: Embrapa Solos; 2011.
- Driscoll RMC, Crilly MS. Subsidence damage to domestic buildings: lessons learned and questions remaining. London: CRC Press; 2000.

- Ene E, Okagbue C. Some basic geotechnical properties of expansive soil modified using pyroclastic dust. *Eng Geol.* 2009;107:61-5. <https://doi.org/10.1016/j.enggeo.2009.03.007>
- Gan JKM, Fredlund DG, Rahardjo H. Determination of the shear strength parameters of an unsaturated soil using the direct shear test. *Can Geotech J.* 1988;25:500-10. <https://doi.org/10.1139/t88-055>
- Gheorghe R, Adia G, Dorin T, Radu B. Engineering properties of Vertisols. *Soil Form Factors Process from Temp Zo.* 2013;12:59-67. <https://doi.org/10.15551/fppzt.v12i1.482>
- Gidigasu SSR, Gawu SK. The mode of formation, nature and geotechnical characteristics of black cotton soils - a review. *Sci Res Essays.* 2013;1:377-90.
- Hakari UD, Puranik SC. Evaluation of index and grain size properties of black cotton soils, Hubballi - Dharwad Municipal Corporation area, Karnataka, India. *Int J Earth Sci Eng.* 2011;4:543-54.
- Hakari UD, Puranik SC. Evaluation of swell potential and identification of expansive and problematic soils in civil engineering works by newly developed matrices based on index and grain size properties. *Electron J Geotech Eng.* 2010;15:1712-26.
- Heping Y, Yongxin Q, Jianlong Z. New development in studies on Ningming expansive soils. *Chinese J Geotech Eng.* 2005;27:981-7.
- IUSS Working Group WRB. World reference base for soil resources 2014, update 2015: International soil classification system for naming soils and creating legends for soil maps. Rome: Food and Agriculture Organization of the United Nations; 2015. (World Soil Resources Reports, 106).
- Jacomine PKT, Cavalcanti AC, Silva FBR, Montenegro JO, Formiga RA, Mélo Filho HFR. Levantamento exploratório - reconhecimento de solos da margem direita do rio São Francisco; Estado da Bahia. Recife: Embrapa-SNLCS: Sudene-DRN; 1979. (Série Recursos de solos, 10).
- Kariuki PC, Woldai T, Van Der Meer F. Effectiveness of spectroscopy in identification of swelling indicator clay minerals. *Int J Remote Sens.* 2004;25:455-69. <https://doi.org/10.1080/0143116031000084314>
- Kong LW, Tan LR. Study on shear strength and swelling-shrinkage characteristic of compacted expansive soil. In: *Unsaturated soils for Asia. Proceedings of the Asian Conference on Unsaturated Soils, UNSAT-ASIA 2000.* Singapore: Unsat; 2000. p. 515-9.
- Kumor MK. Selected geotechnical problems of expansive clays in the area of Poland. *Archit Civ Eng Environ.* 2008;1:75-92.
- Lima GK. Caracterização dos Vertissolos do Nordeste brasileiro. Recife: Universidade Federal Rural de Pernambuco; 2014.
- Miao L, Liu S, Lai Y. Research of soil-water characteristics and shear strength features of Nanyang expansive soil. *Eng Geol.* 2002;55:261-7. [https://doi.org/10.1016/S0013-7952\(01\)00136-3](https://doi.org/10.1016/S0013-7952(01)00136-3)
- Nayak NV, Christensen RW. Swelling characteristics of compacted expansive soils. *Clays Clay Miner.* 1971;19:251-61. <https://doi.org/10.1346/CCMN.1971.0190406>
- Nelson JD, Chao KC, Overton DD, Nelson EJ. *Foundation engineering for expansive soils.* New Jersey: John Wiley & Sons; 2015.
- Paiva SC, Lima MAA, Ferreira MGVX, Ferreira SRM. Propriedades geotécnicas de um solo expansivo tratado com cal. *Matéria.* 2016;21:437-49. <https://doi.org/10.1590/S1517-707620160002.0041>
- Quirk JP. Significance of surface areas calculated from water vapor sorption isotherms by use of the B.E.T equation. *Soil Sci.* 1955;80:423-30. <https://doi.org/10.1097/00010694-195512000-00001>
- Rahardjo H, Aung K, Leong E, Rezaur R. Characteristics of residual soils in Singapore as formed by weathering. *Eng Geol.* 2004;73:157-69. <https://doi.org/10.1016/j.enggeo.2004.01.002>
- Shanker NB, Maruthi G. Use of lime-soil piles for in-situ stabilization of black cotton soils. In: *Proceedings of Indian Geotechnical Conference.* Meerut; 1989. v. 1. p. 149-53.

- Simões de Oliveira AG, Jesus AC, Miranda SB. Estudo geológico geotécnico dos solos expansivos da região do Recôncavo Baiano. In: II Simpósio Brasileiro de Jovens Geotécnicos - II Geojovem; 2006; Nova Friburgo. Nova Friburgo; 2006.
- Taha MR, Hossain MK, Mofiz SA. Behaviour and modeling of granite residual soil in direct shear test. *J Inst Eng Malaysia*. 2000;61:27-40.
- Teixeira PC, Donagemma GK, Fontana A, Teixeira WG. Manual de métodos de análise de solo. 3. ed. rev e ampl. Brasília, DF: Embrapa; 2017.
- Thomas PJ, Baker JC, Zelazny LW. An expansive soil index for predicting shrink-swell potential. *Soil Sci Soc Am J*. 2000;64:268-74. <https://doi.org/10.2136/sssaj2000.641268x>
- Türköz M, Tosun H. A GIS model for preliminary hazard assessment of swelling clays, a case study in Harran plain (SE Turkey). *Environ Earth Sci*. 2011;63:1343-53. <https://doi.org/10.1007/s12665-010-0805-y>
- Wagner LE, Ambe NM, Ding D. Estimating a proctor density curve from intrinsic soil properties. *T ASAE*. 1994;37:1121-5. <https://doi.org/10.13031/2013.28185>
- Ye W, Zhang Y, Chen B, Zhou X, Xie Q. Shear strength of an unsaturated weakly expansive soil. *J Rock Mech Geotech Eng*. 2010;2:155-61. <https://doi.org/10.3724/SPJ.1235.2010.00155>
- Yerima BPK, Galhoun FG, Senkayi AL, Dixon JB. Occurrence of interstratified kaolinite-smectite in El Salvador Vertisols. *Soil Sci. Soc Am J*. 1985;49:462-6. <https://doi.org/10.2136/sssaj1985.03615995004900020038x>
- Yerima BPK, Wilding FG, Calhoun EG, Hallmark CT. Volcanic ash-influenced Vertisols and associated Mollisols of El Salvador: physical, chemical and morphological properties. *Soil Sci Soc Amer J*. 1987;51:699-708. <https://doi.org/10.2136/sssaj1987.03615995005100030026x>
- Yousif AA, Mohamed HHA, Ericsson T. Clay and iron minerals in soils of the clay plains of Central Sudan. *Eur J Soil Sci*. 1988;39:539-48. <https://doi.org/10.1111/j.1365-2389.1988.tb01238.x>
- Zumrawi MME, Eltayeb KA. Laboratory investigation of expansive soil stabilized with calcium chloride. *Int Sch Sci Res Innov*. 2016;10:223-7.
- Zumrawi MME. Pavement design for roads on expansive clay subgrades. *UofKEJ*. 2013;3:52-8.